Essential Readings in Light Metals: Aluminum Reduction Technology.
Edited by Geoff Bearne, Marc Dupuis and Gary Tarcy.

HEAT TRANSFER, THERMAL CONDUCTIVITY, AND EMISSIVITY OF HALL-HEROULT TOP CRUST

Ketil Å. Rye[1], Jomar Thonstad[2] and Xiaoling Liu[3]

SINTEF Materials Technology, Electrolysis Group, N-7034 Trondheim, Norway
Comalco Research Centre, Thomastown, Vic. 3074, Australia

[1] Present address ; Elkem Aluminium AS, N-8651 Mosjøen, Norway.

[2] Laboratories of Industrial Electrochemistry at the Norwegian Institute of Technology, N-7034 Trondheim, Norway.

[3] Comalco Research Centre, Thomastown Vic. 3074, Australia

Abstract

Samples of top crust were prepared in the laboratory, using various bath compositions and temperatures and with variable mixing ratios of alumina/crushed anode cover. The temperature gradient and the heat flux through the crust and the loose alumina mixture were studied, and it was found that the heat flux increased strongly with increasing contents of crushed anode cover in the mixture, due to increased thermal conductivity of the material. Across the air-filled gap between the bath surface and the crust the heat is mainly carried by infra-red radiation, and the investigations showed that the emissivity of the downward-facing crust surface increased slightly with increasing contents of crushed anode cover in the mixture.

Introduction

When cold alumina powder is added to the surface of a molten cryolite bath, a thin layer of frozen bath will immediately cover the alumina grains touching the surface. Since the alumina has insulating properties, this layer will remelt after some time, and the bath will start to permeate the alumina cover as it gradually heats up. A crust is slowly being formed consisting of alumina particles embedded in a mixture of frozen and liquid bath.

A temperature gradient is established through the crust and through the loose alumina resting on top of the crust. If the chemical composition of the melt constitutes a simple eutectic system, the eutectic temperature represents the lowest possible temperature of the liquid phase, and it determines the location of the top of the crust. This implies that in principle the thickness of the crust is determined by the temperature gradient and the eutectic temperature.

Studies of crusts based on the collection of samples from industrial cells have proved to be difficult, because the crust is so inhomogeneous. Voids, cracks and accumulation of carbon dust makes it difficult to obtain representative samples. One is then left with two possible approaches, either to make crust samples in industrial cells under controlled conditions (e.g. by inserting a steel tube in a hole in the crust and add alumina to it), or to make the crust in the laboratory.

One of the earliest comprehensive studies of crust formed in industrial cells was carried out by Volberg et al [1]. On side-break cells a crust thickness between 6 and 9 cm (3 and 12 hours lifetime, respectively) was found, and in point fed cells the crust thickness varied between 9 and 11 cm (48 and 72 hours lifetime). In both types of cells the total thickness of the crust and the loose alumina cover was approximately 15 cm. Three distinct zones were observed in the crust, and chemical analysis showed that compared to the bulk composition of the bath, the crust was enriched in cryolite in the lower parts, while it was enriched in AlF_3 and CaF_2 in the top parts. It was suggested that cryolite is precipitated from the bath as it rises into the crust by capillary action.

The formation and deterioration of crust in industrial cells was recently investigated by Liu et al [2] The work was carried out in two point-fed cells, using secondary alumina mixed with 5-10 wt% crushed anode cover as raw material in one cell, and a mixture containing 50 wt% crushed anode cover in the other. The crushed anode cover was coarse, recycled anode cover with particle sizes up to 15 mm. Chemical analysis showed that the crust was enriched in AlF_3 , except in the bottom layer where the crust had a Cryolite Ratio (CR = mol NaF/mol AlF_3) similar to that of the bath. It was found that the heat flux through the cover formed from the mixture containing 50 wt% crushed anode cover, was larger than through that containing 5-10 wt% crushed anode cover.

The first realistic scheme for making synthetic crust samples in the laboratory was devised by Johnston and Richards [3], and this technique has later been adopted by others, including the present authors [4,5,6,7]. Johnston and Richards studied crust properties such as density, mechanical strength and thermal conductivity. Becker et al [8] used an apparatus which was similar to that of Johnston and Richards. Analysis of the bath phase in the crust showed that the acidity (excess AlF_3) increased when moving upwards into the crust away from the bath. The top of the crust was far more acid than the lower zone (e.g. a CR of 1.40 as opposed to 2.30 in the bath). This observation was the first published experimental confirmation of the observations of Volberg et al [1] Becker et al [9] also measured the mechanical strength of crusts in laboratory cells as well as in industrial cells.

The present work focuses on measurements of the heat transfer and thermal properties of the crust and loose cover using variable bath compositions and temperatures. The loose cover was a blend of primary alumina mixed with varying amounts of crushed anode cover. The crushed anode cover came from the anode butt cleaning process and was a mechanical mixture of top crust, solidified bath and alumina, and it may also contain some solidified metal droplets and carbon particles. The crushed anode cover is customarily used for forming a cover around and on top of newly set anodes.

Experimental

Experimental procedure and equipment

The crusts were grown by adding the mixture of alumina and crushed anode cover inside a thin-walled steel tube that was immersed into the bath which was contained in a graphite crucible. A thorough thermal insulation along the sides of the steel tube gave an approximately uni-directional, vertical heat flux through the crust. The apparatus and procedure for making synthetic crusts have been described in detail in an earlier paper [3].

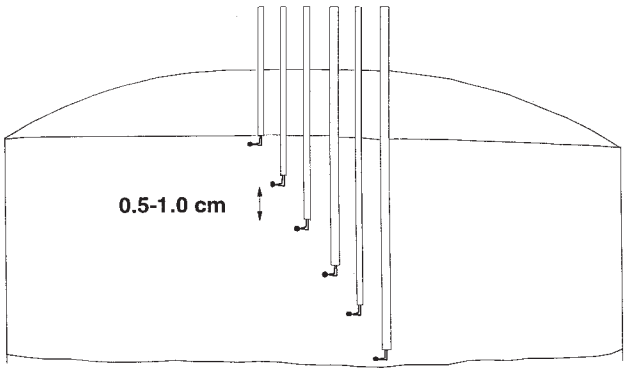

Figure 1. The assembly of thermocouples in the crust. Crust diameter 15 cm.

A heat flow meter (Kemtherm HFM-101, Kyoto Electronics, Japan) was used to monitor the vertical heat flux in the alumina layer on top of the crust, while an assembly of six thermocouples (type S) positioned at various levels in the alumina and crust as shown in Figure 1, was used to monitor the vertical thermal gradient. The temperature at the bottom surface of the crust was measured by inserting a thermocouple through a vertical, ceramic tube. The ceramic tube was inserted prior to the start of the experiment, and hence the crust was grown around it. A rough estimate of the surface temperature could also be obtained from extrapolating the vertical temperature gradient given by the thermocouple assembly.

After the crust was cooled, the thickness and the weight of the crust were measured. Using a diamond saw, a vertical cross-section of the crust was cut and the positions of the thermocouples were noted, which made it possible to calculate the local thermal conductivities of the various zones in the crust.

Experimental parameters

The work was carried out in three separate sets of experiments. In series 1, the aim of the work was to study crust formation with one sample of primary alumina at various bath temperatures and chemical compositions. Six compositions with cryolite ratios (CR = mol NaF/mol AlF_3) ranging from 2.44 to 1.80 were selected, as shown in Table I. Hence, the tests covered baths varying from normal operating baths to what one would call low melting baths. The superheat of the bath, i.e. the difference between the bath temperature and the liquidus temperature, varied according to the changing bath compositions and temperatures.

In series 2, the effect of mixing the alumina with various proportions of crushed anode cover was studied. Two different mixtures of crushed anode cover were used, one with particle sizes ranging from fines to -20 mm (Type A), and one ranging from fines to -8 mm (Type B).

In series 3, an effort was made to study the heat transfer by infra-red radiation across the air-filled gap between the bath surface and the bottom surface of the crust. The aim of this work was to calculate values for the emissivity of the bath surface, and for the crust surface facing the bath. To this means, the temperature difference across the gap had to be measured. The experimental parameters for the three series of the program are given in Tables I, II and III.

Materials

The primary alumina used in the tests was normal smelting grade sandy alumina. The chemical composition of the crushed anode cover material was around 38 wt% Al_2O_3, 7 wt% AlF_3, 3 wt% CaF_2 and balance Na_3AlF_6. A small amount of metallic aluminium was also present in the material. Material Type A contained 10 wt% particles of less than 500 µm, and the maximum particle size was 20 mm. Material Type B contained 40 wt% particles of less than 500 µm, with a maximum particle size of 8 mm.

Table I. Experimental parameters for series 1 of the experimental program.

	Added mixture	CR	CaF_2 [wt%]	Al_2O_3 [wt%]	Bath temp. [°C]	Superheat [°C]	Duration [h]
1	Prim.alumina	2.44	5	3	980	8	4.5
2	Prim.alumina	2.10	5	3	980	32	4.5
3	Prim.alumina	1.90	5	3	980	58	4.5
4	Prim.alumina	2.10	5	3	956	8	4.5
5	Prim.alumina	1.90	5	3	956	34	4.5
6	Prim.alumina	1.80	5	3	900	11	4.5

Table II. Experimental parameters for series 2 of the experimental program, using mixtures of crushed anode cover and alumina.

	Added mixture	CR	CaF_2 [wt%]	Al_2O_3 [wt%]	Bath temp. [°C]	Superheat [°C]	Duration [h]
7	100wt% Type A	1.80	5	3	900	11	4.5
8	50wt% Type A	1.80	5	3	900	11	4.5
9	100wt% Type A	2.07	5	3	985	40	5
10	100wt% Type B	2.07	5	3	956	11	24
11	70wt% Type A	2.07	5	3	985	40	5
12	100wt% Type A	1.55	5	3	895	52	5
13	100wt% Type B	1.55	5	3	895	52	24
14	70wt% Type A	1.55	5	3	895	52	5
15	50wt% Type B	2.07	5	3	956	11	5

Table III. Experimental parameters for series 3 of the experimental program.

	Added mixture	CR	CaF_2 [wt%]	Al_2O_3 [wt%]	Bath temp. [°C]	Superheat [°C]	Duration [h]
16	85wt% Type B	2.10	5	3	956	8	5
17	70wt% Type B	2.10	5	3	956	8	5
18	20wt% Type B	2.10	5	3	956	8	8
19	85wt% Type B	2.10	5	3	956	8	12
20	70wt% Type B*	2.10	5	3	956	8	12
21	20wt% Type B	2.10	5	3	956	8	7

* : A perforated disk of sintered alumina constituted the bottom of the "crust". The crushed anode cover mixture was placed on top of the disk, before the disk made contact with the bath.

Theory

Thermal conduction, convection and radiation

The heat flow through the top crust is mainly determined by the overall thermal conductivities of the crust and the loose alumina powder, and by the total thickness of the cover. At steady state the heat flux through the crust ; $Q_C = \lambda_C (T_B - T_P)$, and the heat flux through the loose alumina ; $Q_A = \lambda_A (T_P - T_S)$ are equal, and in principle the steady state crust thickness, L_C, can be estimated by ;

$$L_C = L_{TOT} \left(\frac{\lambda_A}{\lambda_C} \frac{(T_P - T_S)}{(T_B - T_P)} + 1 \right)^{-1} \quad (1)$$

where L_{TOT} is the total thickness of the crust and loose alumina cover, T_B is the bath temperature, T_P is the lowest possible temperature where liquid bath can exist in the crust, T_S is the surface temperature of the loose alumina, λ_C is the overall thermal conductivity of the crust and λ_A is the overall thermal conductivity of the loose alumina, as shown in Figure 2.

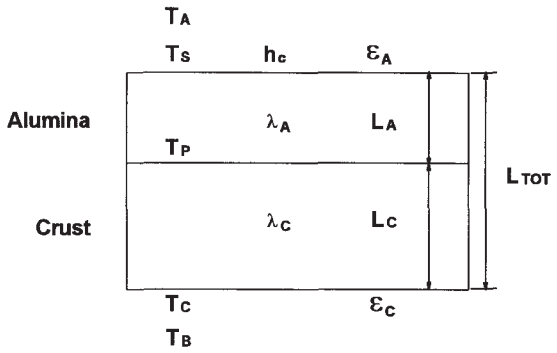

Figure 2. Schematical representation of the crust and loose alumina.
L_A : The thickness of the loose cover resting on top of the crust [m]
L_C : The thickness of the crust [m]
L_{TOT} : The total thickness of the crust and loose cover [m]
T_B : The bath temperature [°C]
T_C : The temperature at the crust surface facing the bath [°C]
T_P : The temperature at the bath front [°C]
T_S : The surface temperature of the loose alumina [°C]
T_A : The ambient temperature [°C]
λ_C : The overall thermal conductivity of the crust [W/mK]
λ_A : The overall thermal conductivity of the loose cover [W/mK]
h_c : The heat transfer coefficient at the loose cover surface [W/m^{2}K]
ϵ_A : The emissivity of the surface of the loose cover
ϵ_C : The emissivity of the crust surface facing the bath

From the surface of the loose cover and into the ambient atmosphere inside the cell hood, the heat is carried by a combination of convection and thermal radiation. The convective heat flux is given by ;

$$Q = h_C (T_S - T_A) \quad \textbf{(2)}$$

where T_A is the ambient temperature and h_C is the convective heat transfer coefficient between air and a flat, horizontal surface of alumina powder.

The radiation heat flux from the surface of the loose cover can be estimated by ;

$$Q = \epsilon_A \sigma \left((T_S + 273)^4 - (T_A + 273)^4 \right) \quad \textbf{(3)}$$

where ϵ_A is the emissivity of the surface of the loose cover and $\sigma = 5.67 \cdot 10^{-8}$ W/m^{2}K^4 is Stefan-Boltzmann's constant. If it is assumed that h_C = 10 W/m^{2}K and ϵ_A = 0.4, equations 2 and 3 show that the radiation heat flux will be dominant for surface temperatures above 350 °C. The value for the convective heat transfer coefficient was estimated in an earlier work [3], but it is not known whether the emissivity of the alumina surface in aluminium smelter cells has ever been measured. Hence, the value of 0.4 was arbitrarily chosen.

Results

The results from stage 1 of the experimental program showed that for crusts made from primary alumina a steady state heat flux was found ranging from 1700 to 1900 W/m^2. The heat flux decreased slightly at lower bath temperatures, and increased at lower CR's.

The thermal conductivity of the crust was calculated from the equation ; $\lambda_C = L_C Q/(T_B - T_P)$, where L_C is the crust thickness, Q is the heat flux, T_B is the bath temperature and T_P is the lowest possible temperature where liquid bath can exist in the crust. In this work T_p was set equal to 725°C. The choice of this value will be discussed in the following.

Similarly, the thermal conductivity of the loose cover was calculated from the equation ; $\lambda_A = L_A Q/(T_P - T_S)$ and the overall thermal conductivity from the equation ; $\lambda_{TOT} = L_{TOT} Q/(T_B - T_S)$. In some cases the surface temperature of the loose cover, T_S, was not measured, and the expression $T_S = Q/h_c + T_A$, where T_A is the ambient temperature and h_C = 10 W/m^{2}K, was substituted for T_S. The expression excludes the thermal radiation, and is valid for the laboratory situation only.

The rate of penetration of bath into the loose cover was recorded by applying a low DC voltage between each thermocouple and the crucible. When the bath front reached the tip of the thermocouple, a signal was recorded. The temperature at the bath front and time since the start of the experiment was noted. In most cases, a plot of the recorded time of arrival of the liquid bath versus the positions of the thermocouples in the crust at times from 0.5 to 2 hours after the start of the experiments presented a linear curve, and the rate of penetration was found by linear regression. In two cases, the curve deviated significantly from linearity, and in those cases the rate of penetration was not calculated.

A crust could not be formed when the added mixture was made up of 100% crushed anode cover of Type A (fines to -20 mm), while a weak, but stable, crust was formed from 100% crushed anode cover of Type B (fines to -8 mm). The crusts made from 100% Type A caved in and dissolved in the bath shortly after addition to the bath surface, while a stable crust was formed when 30 wt% alumina was mixed with the crushed anode cover (of Type A) before addition.

Figure 3 shows the calculated thermal conductivity of the crust versus the cryolite ratio of the bath for different proportions of crushed anode cover of Types A and B in the added mixture. It is readily seen that the thermal conductivity of the crust, and hence also the combined thermal conductivity of the crust and loose cover, increased when crushed anode cover was mixed into the alumina. It is also seen that the crusts formed at lower bath CR's exhibited a higher thermal conductivity.

Tables IV, V and VI show some experimental results. The surface temperature of the loose cover is the temperature shown as T_S in Figure 2, while the temperature at the advancing bath front is the temperature shown as T_P.

Table IV. Results from stage 1 of the experimental program.

	1	2	3	4	5	6
Crust thickness [cm]	6.5	7.5	8.0	7.0	8.0	7.5
Surface temperature, loose cover [°C]	195	195	230	180	210	180
Temperature at bath front [°C]	700	675	665	710	660	700
Heat flux [W/m^2]	1710	1710	1890	1790	1890	1690
Thermal conductivity, loose cover [W/mK]	0.20	0.15	0.15	0.15	0.15	0.15
Thermal conductivity, crust [W/mK]	0.45	0.50	0.60	0.55	0.65	0.70
Thermal conductivity, overall [W/mK]	0.25	0.25	0.30	0.30	0.30	0.30
Rate of bath penetration [mm/min]	0.6	0.4	0.4	0.3	0.3	0.3

Table V. Results from stage 2 of the experimental program.

	7	*8	10	11	13	14	15
Crust thickness [cm]	9.0	8.5	8.0	9.5	9.0	9.5	10
Surface temperature [°C]	260	225	260	250	220	240	235
Temperature at bath front [°C]	655	665	715	680	690	650	730
Heat flux [W/m^2]	2650	2330	3330	2840	3120	2660	3020
Thermal cond. loose cover [W/mK]	0.15	0.15	0.30	0.20	0.20	0.15	0.15
Thermal cond. crust [W/mK]	1.35	1.15	1.15	1.05	1.65	1.50	1.30
Thermal cond. overall [W/mK]	0.50	0.40	0.60	0.45	0.55	0.50	0.50
Rate of bath penetration [mm/min]	0.5	0.4	0.4	0.7	0.5	0.6	0.7

Table VI. Results from stage 3 of the experimental program.

	16	17	18	19	20	21
Crust thickness [cm]	8.5	8.0	7.5	8.5	7.0	9.0
Surface temperature, loose cover [°C]	-	-	-	-	-	-
Temperature at bath front [°C]	635	650	740	695	705	685
Heat flux [W/m^2]	2800	2200	2020	2660	2430	2330
Thermal conductivity, loose cover [W/mK]	0.20	0.15	0.15	0.20	0.25	0.15
Thermal conductivity, crust [W/mK]	1.05	0.75	0.65	1.00	0.75	0.90
Thermal conductivity, overall [W/mK]	0.50	0.40	0.30	0.45	0.40	0.40
Rate of bath penetration [mm/min]	0.9	0.6	0.7	-	-	0.6

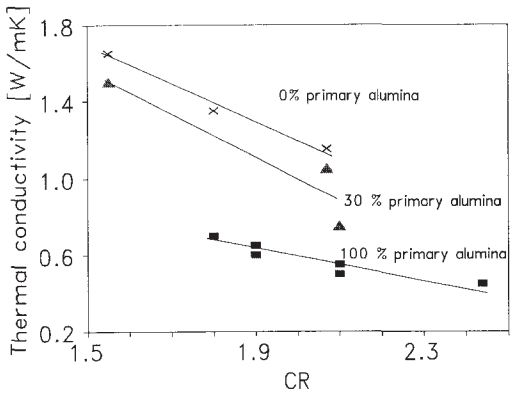

Figure 3. The thermal conductivity of crust for different cryolite ratios (CR) of the bulk bath and different proportions of primary alumina and crushed bath in the added mixture (Types A and B). Lines ; linear regression. Bath additives ; 5wt% CaF_2, 3wt% Al_2O_3.

Table VII gives some data for the heat transfer across the gap and calculated emissivity values for the crust surface facing the bath. The emissivity of the crust surface was calculated from the heat flux, the measured gap height and the temperature difference across the gap. The emissivity of the bath surface was set equal to 1.0, which is close to the value of 0.97 that is indicated by literature data [10] for the emissivity of liquid cryolite, i.e. the liquid cryolite bath acts very closely as a black-body radiator. The crust temperature is the temperature at the crust surface facing the bath, and is given as T_C in Figure 2. The definition of the view-factor is given in the discussion.

The results of tests 19 and 20 indicate that although the increase of the gap height lowers the crust surface temperature, it does not change the heat flux significantly.

Table VII. Experimental data for the radiative heat transfer across the air-filled gap.

	Heat flux [W/m^2]	Bath temp.[°C]	Crust temp.[°C]	Gap height [cm]	View-factor (see text)	Emissivity, crust
16	2800	957	930	1.5	0.8	0.25
18	2020	955	932	1.5	0.8	0.21
18	1960	956	926	1.5	0.8	0.16
19	2660	955	924	1.0	0.9	0.20
19	2620	950	921	1.5	0.8	0.22
19	2640	950	918	3.5	0.6	0.20
20	2310	960	941	1.0	0.9	0.31
20	2430	956	939	1.5	0.8	0.35
20	2370	959	926	2.5	0.7	0.18
21	2360	995	945	2.5	0.7	0.11*
21	2330	955	900	3.5	0.6	0.11*

* : the crust bottom consisted of a plate of sintered α-Al_2O_3

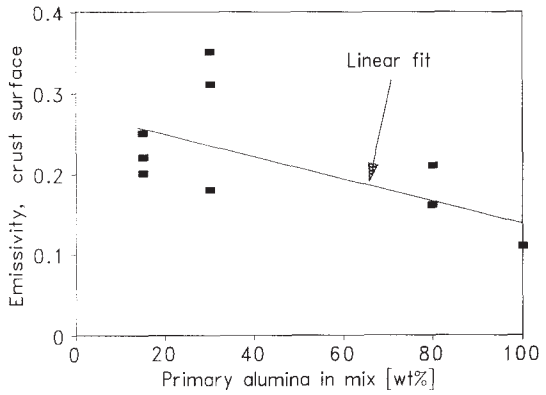

Figure 4. The emissivity of the crust surface facing the bath calculated from the heat flux and the recorded temperature difference across the air-filled gap between the bath surface and the crust.

A plot of the emissivity values for the crust surface is shown in Figure 4. A linear fit of the data indicates that the emissivity decreases with increasing proportions of alumina, but this effect is slight.

Discussion

Emissivity estimates

A simplified theory of heat radiation was used in order to estimate values for the emissivity of crust. At temperatures above the absolute zero a surface will always emit electromagnetic radiation. The net heat transported by radiation between two isothermal, parallel plates of infinite dimensions is given by ;

$$Q = \frac{\sigma \epsilon_1 \epsilon_2}{\epsilon_1 + \epsilon_2 - \epsilon_1 \epsilon_2} \left((T_1 + 273)^4 - (T_2 + 273)^4 \right) \quad [W/m^2] \quad (4)$$

where ϵ_1 and ϵ_2 are the emissivities and T_1 and T_2 are the temperatures of plates 1 and 2 in degrees Celsius.

In the case where the heat-radiating surface can "see" not only the heat-absorbing surface, but also other surfaces, a parameter termed geometrical resistance against heat radiation, R_{res} , is utilized. The geometrical resistance includes the areas of the radiating, the absorbing and the adiabatic surfaces present (i.e the bath surface, the crust underside and the vertical iron tube spanning the gap between the bath surface and the crust underside), and it also includes the so-called view-factor, which is a parameter describing the apparent extent of the hemispherical view that a surface covers as seen from any other surface.

In the case of the laboratory apparatus for crust formation we have one net radiating surface, which is the bath surface, one net absorbing surface, which is the underside of the crust, and one adiabatic surface, which is the cylinder-shaped steel tube in which the crust is formed. The radiation heat flux across the gap is then given by ;

$$Q = \frac{\sigma}{R_{res}} \left((T_1 + 273)^4 - (T_2 + 273)^4 \right) \quad [W/m^2] \quad (5)$$

where R_{res} is given by ;

$$R_{res} = \frac{1 - \epsilon_1}{A_1 \epsilon_1} + R_{res,b} + \frac{1 - \epsilon_2}{A_2 \epsilon_2} \quad (6)$$

and $R_{res,b}$ is given by ;

$$R_{res,b} = \left(A_1 F_{12} + \frac{1}{\frac{1}{A_R F_{R1}} + \frac{1}{A_R F_{R2}}} \right)^{-1} \quad (7)$$

In equations 6 and 7, A_1, A_2 and A_R are the areas of the radiating, absorbing and adiabatic surfaces, respectively. F_{12} is the view-factor between the radiating and the absorbing surfaces, F_{R1} is the view-factor between the adiabatic and the radiating surfaces and F_{R2} is the view-factor between the adiabatic and the absorbing surfaces.

According to VDI-Värmeatlas/11/, the view-factor from the bath surface to the crust bottom for different gap heights in the laboratory apparatus can be found from equation 8 ;

$$F_{12} = \frac{1}{2\tan^2\theta} \left(1 + 2\tan^2\theta - \left(1 + 4\tan^2\theta \right)^{0.5} \right) \qquad \textbf{(8)}$$

where the angle θ is defined as shown in Figure 5.

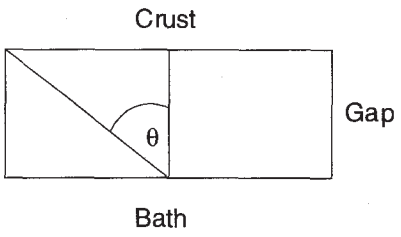

Figure 5. Definition of the angle θ for calculation of the view-factor from bath surface to crust, F_{12}.

In the laboratory furnace, the surfaces of the bath, crust and sidewall are a closed tube where the heat is radiated from the flat circular bottom to the circular top and with an insulated (adiabatic) sidewall. The system is symmetrical, i.e. $F_{R1} = F_{R2}$, and we get ;

$$R_{res,b} = (A_1 F_{12} + 0.5 A_R F_{R1})^{-1} \qquad \textbf{(9)}$$

The view factor from the adiabatic surface to the source, F_{R1}, is different from the view factor from the source to the adiabatic surface, F_{1R}. However, for zero gap height the adiabatic surface can not "see" itself ($F_{RR} = 0$) and we have that $F_{R1} + F_{R2} = 1$. Since $F_{R1} = F_{R2}$ we obtain $F_{R1} = F_{R2} = 0.5$ at zero gap height.

Hence, for small gap heights we assume that $F_{R1} \cong 0.5$, and we get :

$$R_{res,b} = (A_1 F_{12} + 0.25 A_R)^{-1} \qquad \textbf{(10)}$$

For a known geometry, given by the areas A_1, A_2 and A_R, the view factor, the emissivity of the bath surface and the measured heat flux, the emissivity of the crust surface can be estimated from equations 5 to 10.

The main sources of error in the emissivity estimates probably lie in the experimental measurements of the temperature difference between the bath-facing crust surface and the bath surface, and the measurements of the heat flux.

An error of ± 3°C was estimated for the measurements of the temperature difference across the gap, which at maximum error gives a variation of ± 0.03 for the emissivity values given in Table VII. In experimental trials, Comalco has measured deviations of about 20% between different instruments and probes of the Kemtherm heat flux meter.

In addition, the assumption that the sidewall going from the bath surface to the crust was an adiabatic surface and the simplification of the view factor in equation 10, F_{R1}, may be a source of error. Both assumptions give an increasing error for increasing gap heights, as the area of the sidewall exposed to thermal radiation increases with increasing gap height.

Combined with the error in estimating the temperature difference across the gap, the error in the heat flux measurements may give a total error of about ± 30% in the emissivity estimates shown in Table VII.

The temperature at the bath front

The measured temperatures at the advancing bath front given in Tables IV to VI show considerable scatter. In some cases the reported values are well below the lowest possible temperatures where liquid bath can exist in the chemical system Na_3AlF_6-AlF_3-Al_2O_3-CaF_2. The fact that the recorded temperature at the bath front often was below the theoretical limit, indicates that the tip of the thermocouple and the thermocouple wire had a cooling effect on the advancing bath.

The temperature at the bath front was utilized in calculating the overall thermal conductivity of the crust and the loose cover. The proportion of liquid bath at the bath front is very low and the thermal gradient at the bath front is steep. Both factors makes it hard to locate the exact position and the temperature at the top of the crust.

Due to the considerable scatter in the measurements, the recorded temperature at the bath front was considered unsuitable for calculating the thermal conductivity. Hence, rather than using the recorded temperature, the temperature at the bath front was set equal to 725 °C in all experiments. The value 725 °C, which according to Skybakmoen et al [12] is close to the ternary peritectic temperature of the system Na_3AlF_6-AlF_3-Al_2O_3, is about 40 °C higher than the mean value of the measured interface temperatures given in Tables IV to VI.

When the bath contains no CaF_2 the temperature at the bath front should be close to the peritectic temperature of the system Na_3AlF_6-AlF_3-Al_2O_3, which is where all liquid phase would solidify when a melt with a CR higher than 1.67 is cooled. If the bath contains CaF_2, the lowest possible temperature at the bath front should be close to the peritectic point at 688 °C, which according to Lee et al [13] exists in a subset of the system Na_3AlF_6-AlF_3-CaF_2.

If a liquid of a typical industrial composition is cooled in a crucible, the last liquid phase would solidify at the peritectic point. However, if the solid phases that are deposited during cooling are separated from contact with the liquid phase, the liquid will pass the peritectic point and not solidify completely until at the eutectic point. According to Lee et al [13] an eutectic point in the system Na_3AlF_6-AlF_3-CaF_2 can be found at 680 °C.

During the growth of the crust the liquid phase is flowing into the alumina and is continually depositing solid cryolite and alumina. Hence, the liquid at the bath front is separated from the deposited solids, and the liquid at the bath front may pass the peritectic point. The low temperatures recorded at the bath front indicate that this may be the case. However, neither chemical nor instrumental analysis of crust material taken from the top 1-2 mm of synthetic crusts have shown conclusive evidence that the chemical composition of the liquid bath in the crust existed below the peritectic temperature [6].

If the correct temperature at the bath front were 680 °C, which is the eutectic temperature, rather than 725 °C, this would give an approximate 14 - 16 % decrease in the estimated values for the thermal conductivity of the crust, and an approximate 8 - 10 % increase in the values for the thermal conductivity of the loose cover. The values for the overall thermal conductivity of the total cover would not be affected.

Theoretical estimates of the heat flux versus loose alumina thickness

At steady state the heat flux and the thickness of the crust and the loose alumina cover can be estimated if the temperatures, thermal conductivities and total thickness of the cover is known. Using equations 1 to 10 and assuming that steady state has been reached, we can find values for the theoretical heat flux and crust thickness as a function of the loose cover thickness can be found, as shown in Figure 6. For the estimates the following values were used ; h_C = 10 W/m^{2}K, T_B = 950°C, T_P = 725°C, T_A = 50°C, λ_C = 0.4 W/mK, λ_A = 0.2 W/mK, ϵ_C = 0.3 and ϵ_A = 0.4. The emissivity of the bath surface was set equal to 1.0. For validation, Figure 6 also shows some measurements of heat flux vs. alumina depth reported by Richards[14], which were performed on un-hooded industrial cells.

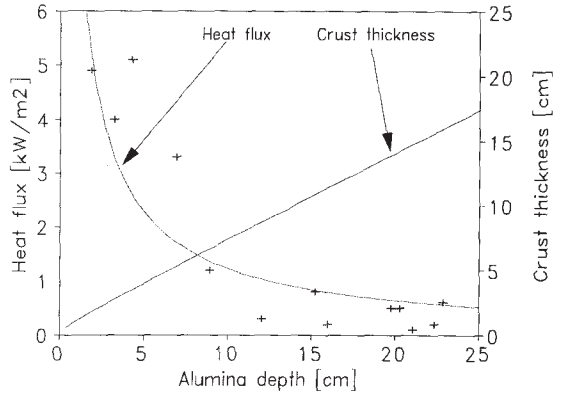

Figure 6. Theoretical estimates of the steady state heat flux and crust thickness as a function of the thickness of the loose alumina cover. Input ; h_C = 10 W/m^{2}K, T_B = 950°C, T_P = 725°C, T_A = 50°C, λ_C = 0.4 W/mK, λ_A = 0.2 W/mK, ϵ_C = 0.3 and ϵ_A = 0.4. The points (+) are measured data from industrial cells reported by Richards [14].

The positions of the lines shown in Figure 6 change little with normal variations in the input parameters, and the shapes of the curves do not change. Figure 6 indicates that the thickness of the loose alumina cover should not be less than 6-8 cm, while an increased thickness of the loose cover to more than 10-12 cm has little effect on the heat flux, but gives an increasing crust thickness.

Conclusion

Mixing the alumina with crushed anode cover gave an increased heat flux due to the higher thermal conductivity of the crusts which were formed from this material. A stable top crust could not be formed if the added mixture consisted of 100 wt% crushed anode cover of Type A, which had a maximum particle size of 20 mm, but a stable crust was formed if the same crushed anode cover was mixed with 30 wt% alumina powder.

Across the air-filled gap between the bath surface and the underside of the crust the heat is transferred by radiation. Emissivity values in the range 0.11-0.35 were found for the bath-facing crust surface.

Acknowledgements

The authors at SINTEF Materials Technology and the Laboratories of Industrial Electrochemistry at the Norwegian Institute of Technology gratefully acknowledges financial support from Comalco Research Centre for a joint project, and we also acknowledge the permission to publish this work.

Nomenclature

ϵ_A	-	The emissivity of the surface of the loose cover
ϵ_C	-	The emissivity of the crust surface facing the bath
ϵ_1, ϵ_2	-	General emissivities
λ_A	-	Overall thermal conductivity, loose cover [W/mK]
λ_C	-	Overall thermal conductivity, crust [W/mK]
σ	-	The Stefan-Boltzmann constant
θ	-	Angle for calculation of F_{12}
h_c	-	Heat transfer coefficient, loose cover [W/m^{2}K]
A_1,A_2,A_R	-	General surface areas
F_{12}	-	View-factor between the bath surface and the crust
F_{R1}	-	View-factor from the sidewall to the bath surface
F_{1R}	-	View-factor from the bath surface to the sidewall
F_{R2}	-	View-factor from the sidewall to the crust
L_A	-	Thickness of the loose cover [m]
L_C	-	Thickness of the crust [m]
L_{TOT}	-	Total thickness of the crust and loose cover [m]
T_A	-	Ambient temperature [°C]
T_B	-	Bath temperature [°C]
T_C	-	Surface temperature, crust bottom [°C]
T_P	-	The temperature at the bath front [°C]
T_S	-	Surface temperature, loose cover [°C]
T_1,T_2	-	General temperatures
Q	-	Heat flux [W/m^2]
Q_A	-	Heat flux through the loose cover [W/m^2]
Q_C	-	Heat flux through the crust [W/m^2]
R_{res}	-	Geometrical resistance against heat radiation
$R_{res,b}$	-	Subterm, geometrical resistance

References

1. A.A. Volberg, E.L. Sukhanov, A.I. Belyaev. "Structure and thermophysical properties of surface crust formed on industrial aluminium cells." Izv. Nauk. SSSR. Met. Gorn. Delo. No.5 (1964) pp. 45-56. (Russian text)

2. X. Liu, M.P. Taylor, S.F. George. "Crust formation and deterioration in industrial cells." TMS Light Metals 1992, pp. 489-494.

3. T.J. Johnston and N.E. Richards, "Correlation between alumina properties and crusts", TMS Light Metals 1983, pp. 623-639

4. T. Eggen, S. Rolseth, K. Rye, J. Thonstad. "Alumina crusting in cryolitic melts. Part I : Penetration of molten electrolyte into alumina." TMS Light Metals 1992. pp. 495-502.

5. K.Å. Rye. "Alumina crusting in cryolitic melts. Part II : Bulk properties of crust." TMS Light Metals 1992 pp. 503-509.

6. K.Å. Rye. "Crust formation in cryolite-based baths." Dr.Ing. Thesis #22 1992. University of Trondheim, NTH.

7. K.Å. Rye. "In-situ measurements of the thermal conductivity of laboratory made Hall-Heroult crusts." Proc. 7'th Al. Symp. Banska Bystrica, Slovakia 1993. pp. 293-300.

8. A.J. Becker, T.R. Hornack and R.M. Mazgaj, "Hardness of crust and properties of crust". Unpublished results presented at the 114'th AIME Annual Meeting, New York, February 24-28, 1985, and Internal Reports, Alcoa Laboratories.

9. A.J. Becker, T.R. Hornack, T.J. Steinbeck, "In-situ properties of crusts formed with five ores in a Soderberg smelting cell," TMS Light Metals 1987, pp. 41-50.

10. Battelle Inert Electrodes Program ; "Final report on the PNL program to develop an alumina sensor." US. Dept. Energy Contract DE-AC06-76RLO 1830 (1992) p. 4.1

11. "Bestimmung von Einstrahlzahlen." VDI-Wärmeatlas. VDI-Verlag GmbH, Düsseldorf, Germany, 3.ed (1977) p. Kb 5.

12. E. Skybakmoen, A. Solheim, and A. Sterten, "Phase Diagram for the System Na_3AlF_6-Li_3AlF_6-AlF_3-Al_2O_3. Part II: Alumina Solubility," Light Metals 1990, pp. 317-323.

13. S.S. Lee et al. "Determination of melting temperatures and Al_2O_3-solubilities for Hall cell electrolyte compositions." TMS Light Metals 1984, pp. 841-855.

14. N.E. Richards. "Alumina in smelting." Proc.13'th Int. Course on Process Met. of Aluminium. Trondheim, Norway 1994, p. 3.40.